

Statistical monitoring of functional data using the notion of Fréchet mean combined with the framework of the deformation models

G. I. Papayiannis^{*a,c}, S. Psarakis^b, and A. N. Yannacopoulos^c

^aMathematical Modeling and Applications Laboratory, Section of Mathematics, Hellenic Naval Academy, Piraeus, Greece

^bDepartment of Statistics, Athens University of Economics & Business, Athens, Greece

^cStochastic Modeling and Applications Laboratory, Department of Statistics, Athens University of Economics & Business, Athens, Greece

November 18, 2021

Abstract

The aim of this paper is to investigate possible advances obtained by the implementation of the framework of Fréchet mean and the generalized sense of mean that it offers, in the field of statistical process monitoring and control. In particular, the case of non-linear profiles which are described by data in functional form is considered and a framework combining the notion of Fréchet mean and deformation models is developed. The proposed monitoring approach is implemented to the intra-day air pollution monitoring task in the city of Athens where the capabilities and advantages of the method are illustrated.

Keywords: control charts; deformation models; Fréchet mean; functional data; shape invariant model;

1 Introduction

The problem of monitoring non-linear profiles has recently attracted the attention of the community of statistical process control. This is a consequence of the evolution and development of more elaborate and complex statistical monitoring schemes allowing for dynamical and functional data structures containing and revealing important useful information concerning the

*Corresponding author: Patission Str. 76, Athens, 10434, Greece. E-mail: gpapayiannis@aueb.gr

process in question. The resulting functional data (and their increased complexity) is an issue that at a first stage can be handled either by the application of non-linear models or by non-parametric or semi-parametric models (e.g. kernel-based estimators, wavelets, etc.). However, as far as statistical control is concerned, for these functional models the classical control tools may not be appropriate (partly because of their functional nature and partly because the output of such models may not be appropriately accommodated in a vector space framework). This fact imposes the need for development of new monitoring mechanisms. Particularly, in the area of non-linear profile monitoring, several approaches have been proposed in the later years, e.g. non-linear regression approaches Williams et al. (2007), non-parametric regression Qiu et al. (2010), interpolation approaches Fassò et al. (2016), wavelets Chicken et al. (2009); McGinnity et al. (2015), principal components analysis Shiau et al. (2009), support vector machines Moguerza et al. (2007) and others. The aforementioned approaches attempt (through modifications in the modeling procedure, but still relying in the current setting of process control theory and practice) to extend the current monitoring tools in order to better treat the new modeling setup accommodating certain of the salient features of the data in question (such as functional dependence etc).

However, there is an important issue that requires further investigation. That is the actual definition of the typical (or the so called *in control* (IC)) behaviour of the object under study. The main problem here is that the standard approaches have been developed for data that can be considered as points of a finite dimensional Euclidean space (\mathbb{R}^d) of suitable dimensionality related to the number of features under consideration, possibly carrying a correlation structure or displaying variability which is modelled essentially under the assumption that the data are distributed according to probability laws similar or sufficiently close to a Gaussian law. On the context of functional data the above setting is not appropriate for a number of reasons. To name just a few the finite dimensionality assumption is no longer sufficient as the data in question are infinite dimensional, the correlation structure between the data may not suitably modelled within the normality assumption but a modeling of the functional form of the procedure generating the observed data may offer a more appropriate vehicle for quantifying the dependencies and complex correlation structures between the data, and, importantly, in many cases of interest the observed data may no longer be understood as elements of a vector space but may be elements of a space with nonlinear or convex structure, for example elements of a general metric space. As an example of the last case one could mention e.g. data in the form of covariance matrices or data in the form of curves of a particular form (e.g. convex curves or increasing curves).

Recently, Cano et al. (2015) initiated the development of a more appropriate framework for dealing with functional data of the above type using tools from the statistical shape theory. The aim of this work is to revisit and further extend their approach, with an emphasis on the appropriate definition of the IC behaviour of the statistical process under study, through an appropriate notion of mean for metric space valued data, the Fréchet mean, combined with the framework of deformation models. The approach we propose and develop is quite general and can be applied to any functional object (e.g. curves, surfaces, etc.), however we restrict ourselves to the case of curves in order to properly motivate the proposed methodology. Advantages and capabilities of the proposed approach are illustrated and discussed in Section 4 where air-pollution status in the area of Athens is monitored through the proposed scheme with very interesting results.

2 Background & Preliminaries

2.1 Motivation

Nonlinear profiles are not objects that can be efficiently described as elements of a vector space. Consider as a motivating example a sigma shaped profile. Clearly, considering the profile as discrete observations in \mathbb{R}^n for a suitable n is not a very good strategy as the shape of the profile introduces strong correlations of a specific nature which may not conveniently modelled in this framework. A general functional approach can be a better strategy, but then we also need to worry concerning the qualitative features of the profiles in question. For example if we monitor a sigma shaped profile, linear combinations of various sigma shaped profiles may fail to satisfy the fundamental qualitative properties of the profile, i.e. being sigma shaped. A possible modeling approach for such a case could be to look for models within the set $M = \{f(\cdot; \theta) : \theta \in U \subset \mathbb{R}^d\}$ where f is a given sigma shaped function and θ are parameters chosen in a suitable set U . Observed profiles can be considered as random elements from M . The mean behaviour of a sample of observed profiles (equiv. a sample of random elements from M) and its variance must be properly defined, to be used in the monitoring procedure. Reflecting on the form of the standard estimators for the mean we see that these are based on the linearity of the set M . However, the set M clearly does not enjoy a linear structure. Nevertheless, it can naturally be endowed with a metric space structure (M, d) , or sometimes even a Riemannian manifold structure. We may then consider the observed profiles as random elements of this metric space (M, d) (hereafter simplified to M) and seek for a meaningful way, free from linearity assumptions, in order to describe such observations and develop process monitoring schemes

suitable for metric space valued data. The above situation is not particular to sigma shaped profiles, problems related to monotonic or convex profiles or even batch data which can be modelled as probability distributions (or measures) can be more naturally considered as elements of appropriate metric spaces, not enjoying a linear structure.

The concepts of the Fréchet mean and variance constitute the perfect framework for this task. In what follows, we recall certain fundamental properties of the Fréchet mean and variance, necessary in order to proceed with the main task of this paper which is to propose a monitor framework for functional data profiles in Section 3.

2.2 The notion of Fréchet mean

The typical notion of mean may not be applicable when working on spaces which do not enjoy a vector space structure (e.g. linearity, for example data in \mathbb{R}^d) but have to be considered as elements of a more general metric space. For specific examples one may consider data corresponding to curves or surfaces of a special form (e.g. s-shaped curves, data with a monotonicity of ordering structure), data in the form of matrices of specific form (e.g. positive definite matrices) or data in the form of probability distributions or measures. A major problem arising in such cases is that the standard notion of mean in terms of a weighted average or linear integral over a measure may fail to enjoy important qualitative properties that the data do (defining their membership to the chosen metric space) i.e. the standard averaging procedure may produce an object which does not belong to the same metric space as the data. This clearly leads to conceptual issues in the interpretation of the mean, and in the context we consider here in its use when trying to quantify the IC behaviour of a statistical process.

A very natural generalization of the mean in metric spaces, without a vector space structure, has been developed by Maurice Fréchet (the original publication is Fréchet (1948)) leading to a more general notion of mean, called the *Fréchet mean*. Unlike the usual definition of the mean, the Fréchet mean provides a meaningful sense of the mean element even in spaces where the vector space structure is absent (see e.g. Izem et al. (2007)).

Let (M, d) be a metric space, consider a suitable (probability) measure ν on M and define the *Fréchet function* $\Phi : M \rightarrow \mathbb{R}_+$ as

$$\Phi(y) = \mathbb{E}[d(y, x)^2] = \int_M d(y, x)^2 d\nu(x) \quad (1)$$

for every $y \in M$. The value $\Phi(y)$ represents the mean squared deviance (under the metric sense provided by d) of the element y from all elements $x \in M$, sampled with the probability measure ν . If ν is a discrete measure, supported on the points $x_i \in M$, then $\Phi(y)$ can be considered

as the average distance of the point $y \in M$, from the cloud of points $x_i \in M$, $i = 1, \dots, n$, described by ν , and the integral defining the Fréchet function is replaced by a suitable weighted sum, using an appropriate set of weights $w = (w_1, \dots, w_n) \in \Delta^n$, where by Δ^n we denote the n -dimensional unit simplex.

For the purpose of this paper, we will assume that $X = \{x_1, \dots, x_n\} \subset M$ is a discrete set of points, sampled from a probability distribution ν on M and consider the corresponding Fréchet function Φ_X . We define the *Fréchet mean set* of X , by $E_F(X) := \arg \min_{z \in M} \Phi_X(z)$, i.e. as the set of points on the space which minimize the function Φ_X , and the *Fréchet variance* $\tilde{V}_F(X)$, as $\tilde{V}_F(X) := \Phi_X(\bar{X}_F)$ for any $\bar{X}_F \in E_F(X)$. Consequently, we have that $\bar{X}_F \in E_F(X)$ if and only if it holds that $\Phi(\bar{X}_F) = \inf_{y \in M} \Phi(y)$, and as a result we get that $\tilde{V}_F(X) = \Phi(\bar{X}_F)$. The set $E_F(X)$ may not be a singleton, i.e. there may be more than one Fréchet means, depending on the properties of the metric space M , nevertheless, the Fréchet variance is well defined (i.e. unique) even in such cases. However, for most cases of practical interest e.g. in certain Riemannian manifolds, deformation models or shape spaces the Fréchet mean is uniquely defined Le & Kume (2000); Afsari (2011); Arnaudon et al. (2013); Petersen et al. (2019). These are the cases we will focus on in this work. In such cases the Fréchet mean may be considered as the characteristic or average behaviour of the set of points X , often called the Riemannian center of mass (if M enjoys a Riemannian structure) reflecting the analogy with mechanics. Moreover, if the underlying measure ν is not known, the Fréchet mean can be used for inference schemes for the sample, using estimators based on this notion, using appropriately chosen weights (for example $w_i = \frac{1}{n}$ etc) Papayiannis & Yannacopoulos (2018). We close this brief reminder of the Fréchet mean by noting that if M is a Euclidean space, then the notion of the Fréchet mean coincides with the standard definition of the mean. In general metric spaces M the calculation of the Fréchet mean reduces to a variational problem that can be treated using the techniques of the calculus of variations Kravvaritis & Yannacopoulos (2020). Often, the modeling needs do not require the use of a general abstract metric space, but require metric spaces of special forms which may be expressed in terms of explicit representations such as for instance deformation models or shape models. The use of such models is in most cases ideal for the treatment of the nonlinear profiles problem, as it allows for the mathematical description of particular shapes and forms of the ideal nonlinear profile. The calculation of the Fréchet mean within this general class of models is greatly facilitated, turning the Fréchet mean into a powerful statistical tool.

We now return to the statistical process control context. Recalling that we consider all observed items (e.g. profiles) as random elements of an appropriate metric space M , we consider

the case where the observations $X = \{x_1, x_2, \dots, x_n\} \subset M$ are available. Certain of these elements can be considered as belonging to an IC stage. Assuming that the elements IC stage can be characterized as belonging to a subset of M , which is specified in terms of the support of a probability measure ν we may define a relevant Fréchet function for the IC measurements. Approximate M by the discrete sample X and the measure ν by a discrete measure $w = (w_1, w_2, \dots, w_n)'$ member of the n -dimensional unit simplex $\Delta^n = \{w \in \mathbb{R}^n : \sum_{j=1}^n w_j = 1, w_n \geq 0, \forall j\}$. The later could be interpreted as the observed relative frequencies of the IC measurements under consideration or depending the application the weights may depend on sensitivity parameters which optimal tuning allows for better ability in detecting significant evidence (in Section 3 we discuss this matter where the Fréchet mean weights depend on the exponential weighting parameter). Under this perspective, the *modified Fréchet function* is expressed as

$$\Phi_{IC}(y) = \sum_{j=1}^n w_j d^2(y, x_j) \quad (2)$$

for any point $y \in M$. Clearly, the minimizer of the modified Fréchet function is the most representative member of M for the IC behavior under the metric sense of d , while the achieved minimal value of this function is the Fréchet variance. Then, the Fréchet mean or Fréchet barycenter with respect to the collection of IC observations $\{x_1, x_2, \dots, x_n\}$ is defined as

$$\bar{x}_{IC} = \arg \min_{y \in M} \Phi_{IC}(y) = \arg \min_{y \in M} \sum_{j=1}^n w_j d^2(y, x_j). \quad (3)$$

The uniqueness of the Fréchet mean in the later form depends highly on the choice of the metric d and certain cases have been investigated in Afsari (2011); Arnaudon et al. (2013). Moreover, asymptotic results regarding the random behaviour of the Fréchet mean and extensions of the classical analysis of variance have been studied in Jung et al. (2012); Dubey & Müller (2019).

2.3 Deformation models

Deformation models have been proved a very popular approach in functional statistics. The random elements (data) are assumed to be elements of a metric space of functions, and *deformation models* quantify dissimilarities between functional data through appropriate parameterizations of their shapes. Each realization of such a random element can be considered as a random deformation of a typical element (or shape) with a measure of this deviation characterizing the particular random element in question. Formally, the random elements in a the framework of deformation models are elements of a set $M = \{f \circ T : T \in V\}$ where f is a deterministic function (often to be specified) characterizing the typical (average) shape and $T(\cdot) = T(\cdot, \omega)$ is

a random deformation typically chosen from a vector space V so that the composition $f \circ T(\cdot, \omega)$ generates a random element from M , satisfying certain qualitative features. Hence, each random element is parameterized in terms of the realization of $T \in V$.

This type of statistical modeling have found several applications in practice so far, e.g., in image and signal processing Bigot et al. (2009, 2011), in analysing point processes Panaretos et al. (2016), in medicine Papayiannis et al. (2018), in electric energy prediction Kampelis et al. (2020), etc. The reason behind the growing popularity of this approach is that although fully non-parametric approaches seem very tempting in theory, in practice they rarely can be used for statistical inference when comparisons are needed.

Let us focus on the specific case where the random elements in M corresponds to curves $f : I \rightarrow \mathbb{R}$ where $I \subset \mathbb{R}$ is a given interval. Without loss of generality we may consider $I = [0, 1]$ as corresponding to a time interval with the function $t \mapsto f(t)$, $t \in I$ describing the random temporal evolution of some quantity of interest. Consider two curves $t \mapsto f(t)$, $t \mapsto g(t)$ with g being the reference curve. We are interested in quantifying differences/dissimilarities of f from the reference curve g . Clearly, assuming that $f, g \in M \subset L^2(I)$, a rough measure quantifying difference between the two curves could be the distance $d(f, g) := \|f - g\|_2$, however this value does not provide any qualitative interpretation regarding the specific features with respect to which the two curves differ. The framework of deformation models contributes exactly to this part, i.e. considering appropriate parameterizations to sufficiently allocate the deviance between the objects to certain features related to their shapes, and considering in more detail the actual intrinsic structure of the metric space M , rather than the ambient vector space $L^2(I)$.

Quite a general deformation model has been studied recently in Panaretos et al. (2016), modeling separately *amplitude* and *phase* characteristics. Under this modeling perspective, the shape relation between curves f and g is expressed as

$$f(t) = (\Lambda \circ g \circ \Pi^{-1})(t) + \epsilon(t) = \Lambda(g(\Pi^{-1}(t))) + \epsilon(t) \quad (4)$$

where $\Pi : I \rightarrow I$ for $I \subset \mathbb{R}$ denotes the *phase operator* or *phase deformer* and $\Lambda : L^2(I) \rightarrow L^2(I)$ denotes the *amplitude operator* or *amplitude deformer* and $\epsilon(t)$ the residuals, i.e. the aspects of curve f that cannot be efficiently captured through a deformation of g under this shape modeling approach. Under certain parameterization approaches, the above general deformation model can be represented in parametric form through the equation

$$f(t) = \hat{f}(t; \gamma, \xi) + \epsilon(t) = (\Lambda_\gamma \circ g \circ \Pi_\xi^{-1})(t) + \epsilon(t) = \Lambda_\gamma(g(\Pi_\xi^{-1}(t))) + \epsilon(t) \quad (5)$$

where $\Lambda : \Theta_\Lambda \times L^2(I) \rightarrow L^2(I)$ and $\Pi : \Theta_\Pi \times I \rightarrow I$ for $I \subset \mathbb{R}$ denote the parametric versions of the amplitude and phase deformaters which characteristics are quantified by the parameters γ (amplitude) and ξ (phase) respectively, and $\Theta_\Lambda, \Theta_\Pi$ denote the corresponding parameter spaces (e.g. subsets of \mathbb{R}^{p_Λ} and \mathbb{R}^{p_Π} respectively, with $p = p_\Lambda + p_\Pi$ denoting the total number of the deformation parameters used). Note, that the inverse of the phase deformer $\varphi := \Pi^{-1}$ in literature is also referred to as the *time-warping function* and several modeling approaches of it have been considered especially through the concept of the shape invariant model (see e.g. Kneip & Engel (1995); Wang et al. (1997); Gervini & Gasser (2004)). Since the phase deformer distorts the time domain, should satisfy certain properties like monotonicity, continuity, invertibility, etc. in order to provide a meaningful result. Note that, if only affine deformations are considered both on amplitude and phase, the classical shape invariant model is recovered, i.e. consider $\Lambda(z) = \alpha z + b$ and $\Pi(s) = \kappa s + \zeta$, then

$$f(t) = b + \alpha g\left(\frac{t - \zeta}{\kappa}\right) + \epsilon(t). \quad (6)$$

Therefore, even in the case of a deformation model based on affine distortions, each parameter quantifies certain deviance aspects providing a more complete picture of comparison between curves f and g . It is important to note here that although the distortions are linear the resulting shape model is not a member of a vector space.

The deformation models beyond the qualitative interpretation they offer to the deviance between two different objects (curves in our case), they provide a very convenient framework for the calculation of the Fréchet mean. As we already discussed, the computation of the Fréchet mean among different curves is equivalent to solving a variational problem which even in the “simple” cases (e.g. smooth functions) the minimization task could be proved really challenging and computationally demanding. The use of a particular class of deformation models to parameterically describe (calibrate) the deviation of a particular curve from the one considered as the most typical, reduces the variational problem to a fitting problem. By this mean, a semi-parametric characterization of the Fréchet mean is possible, and given that the modeling approach is plausible (this corresponds to the selection of an appropriate class of deformation model depending the problem at hand), the Fréchet mean is approximated with much lower computational effort and without the need to discretize the problem.

3 A monitoring framework for functional profiles

In this section we present the proposed monitoring approach for functional data representing nonlinear profiles. First, we describe Phase I of the monitoring mechanism which consists of the characterization of the in control (IC) behaviour by combining the notion of Fréchet mean and the framework of the deformation models. Next, we present Phase II of the procedure where an EWMA-type chart is developed for monitoring functional data using deformation models. Finally, as a case of particular interest the shape invariant deformation model is examined and appropriate monitoring schemes are proposed.

3.1 Estimation of the IC behaviour

Consider the case where n functional objects are available, e.g. a set of curves

$$\mathcal{F} := \{f_1, f_2, \dots, f_n\} \subset M \subset V,$$

providing evidence of IC behaviour regarding the statistical process under study, where M is a metric space and V an ambient function vector space, e.g., $L^p(I)$ or a suitable Sobolev space $W^{s,p}(I)$. For example, in medicine these curves could represent the daily evolution of blood pressure from subjects which have been characterized as non-hypertensives and can be estimated by using any non-parametric modeling approach, e.g., kernel-based estimators Wand & Jones (1994); Ramsay & Silverman (2007), splines Wahba (1990), wavelets Chui (2016), etc. It is important at the first step of the statistical monitoring mechanism, to provide a condensed estimation regarding the typical behaviour of subjects that are characterized as IC in order to define a reference object for comparison. The set \mathcal{F} will be used as a training set in order to estimate the typical curve that represents the mean behaviour of what is considered as IC status. The notion of Fréchet mean described in Section 2.2 can be used to provide an estimate of the mean curve, since $\{f_j\}_j$ do not necessarily belong to a vector space, i.e. the typical notion of mean is not applicable.

Depending on the application, certain assumptions regarding the space we work in has to be made. The most usual approach is to consider that all objects under study are members of the ambient space. Without loss of generality set $V = L^2(I)$ (the Lebesgue space of square integrable functions), i.e. $f_j \in L^2(I)$ for all $j = 1, 2, \dots, n$, and consider the corresponding $L^2(I)$ norm $\|f_i - f_j\|_2 = \left(\int_I |f_i(t) - f_j(t)|^2 dt\right)^{1/2}$ as the dissimilarity between the curves f_i, f_j . Therefore, if one desires to derive a fully non-parametric estimate of the mean IC behaviour represented by \mathcal{F} within this framework one may seek for the mean within the $L^2(I)$ framework.

Eventhough this problem is tractable, the resulting mean may fail to enjoy certain important qualitative properties which must hold for the elements of M , hence this mean may not be a suitable representation of the typical IC behaviour.

To remedy this situation the shape modeling framework discussed in Section 2.3 is now implemented, where combined with the notion of Fréchet mean provides, beyond a reference object, several aspects regarding the acceptable deviations of the shape characteristics that are taken into account between the objects under comparison, which may prove extremely useful for the determination of the monitoring status of newly sampled objects. In particular, a standard assumption that is made is that all objects under study are of the same nature, i.e. there is a certain underlying shape and each object's shape can be expressed efficiently as a deformation of it with respect to certain features of the shape. Such approaches have been investigated in literature either from the perspective of differential geometry (see e.g. Goodall (1991); Kendall et al. (2009); Small (2012) or from the perspective of statistical shape modeling (see e.g.. Kneip & Engel (1995); Gervini & Gasser (2004); Bigot et al. (2013)). However, to the best of our knowledge such a framework has not yet been proposed to the field of statistical process control.

The amplitude-phase deformation model (Panaretos et al. (2016)) discussed earlier offers a quite general deformation framework. Consider that each curve f_j in the train set \mathcal{F} can be sufficiently modeled as a deformation of the mean curve f_{IC} (not known yet) as shown in (5) with deformation parameters $\theta_j = (\gamma_j, \xi_j)$ and substituting g with f_{IC} . It is clear that amplitude and phase distortions of the curve f_j comparing to the reference (Fréchet mean) curve f_{IC} are captured by the deformaters $\Lambda_j = \Lambda(\cdot; \gamma_j)$ and $\Pi_j = \Pi(\cdot; \xi_j)$ and quantified by their respective parameters γ_j and ξ_j . However, the deformation parameters cannot be chosen unless the Fréchet mean is defined. Under the current modeling approach, a semi-parametric expression of the mean can be obtained through averaging. In particular, reversing the modeling of each curve as a model of the Fréchet mean with respect to each curve f_j we obtain the expression

$$f_{IC} = \hat{f}_{IC,j}(\theta_j) + \eta_j = \Lambda_j^{-1} \circ f_j \circ \Pi_j + \eta_j \quad (7)$$

where $\eta_j := \Lambda_j^{-1} \circ \epsilon_j \circ \Pi_j$ denotes the distorted error term related to the estimation error relying on the observation from only the curve f_j . The mean curve f_{IC} must be chosen in such a manner that satisfies the barycenter property, i.e. being simultaneously so close and so far from all the elements in the set \mathcal{F} . Therefore, a standard requirement that has to be met is that the average of the residuals η_j among all curves, for each time instant $t \in I$, must be zero, i.e. $\frac{1}{n} \sum_{j=1}^n \eta_j(t) = 0$ for all $t \in I$. As a result by properly averaging every possible model of f_{IC} as

a deformation of each $f_j \in \mathcal{F}$ we obtain the following semi-parametric expression of f_{IC}

$$\hat{f}_{IC}(\boldsymbol{\theta}) = \frac{1}{n} \sum_{j=1}^n \hat{f}_{IC,j}(\theta_j) = \frac{1}{n} \sum_{j=1}^n \Lambda_j^{-1} \circ f_j \circ \Pi_j \quad (8)$$

where $\boldsymbol{\theta} = (\boldsymbol{\gamma}, \boldsymbol{\xi})'$ with $\boldsymbol{\gamma} = (\gamma_1, \dots, \gamma_n)'$ stands for the amplitude deformation parameters and $\boldsymbol{\xi} = (\xi_1, \dots, \xi_n)'$ stands for the phase deformation parameters. Clearly, what is represented in (8) is not the Fréchet mean, but the parametric family depending on $\boldsymbol{\theta}$ which will be used to approximate the Fréchet mean of the set \mathcal{F} . The optimality criterion under which the parameter vector $\boldsymbol{\theta}$ will be chosen, depends on the metric sense d_M under which we wish to derive the mean element. As a result, and keeping in mind the Fréchet function defined in (2), the optimal parameter vector $\boldsymbol{\theta}_*$ is obtained as the solution to the minimization problem

$$\boldsymbol{\theta}_* := \arg \min_{\boldsymbol{\theta} \in \mathfrak{D}} \frac{1}{n} \sum_{j=1}^n d_M^2(f_j, \hat{f}_{IC}(\boldsymbol{\theta})) \quad (9)$$

where \mathfrak{D} stands for the subset of \mathbb{R}^{np} in which the parameter vector $\boldsymbol{\theta}$ lies. Depending on the deformation models that are chosen, certain centrality requirements may be asked for the chosen parameters to satisfy. In the case of the amplitude-phase model, standard requirements for the parameters may be any constraints induced by the centrality properties $\mathbb{E}[\Lambda_j] = \mathbb{E}[\Pi_j] = Id$.

It is evident that this semi-parametric approach provides additional advantages as compared to a fully non-parametric estimation of the mean curve. The most important is that besides the mean estimate, one can obtain a picture regarding acceptable deviance levels concerning the shape features that the adopted deformation model takes into account. The later can be represented/quantified either in terms of the deformation functions or in terms of the individual parameter values. Such information can be derived in the following manner. Let us denote by $f_0 := f_{IC}(\boldsymbol{\theta}_*)$. Then, for each f_j in \mathcal{F} solve the registration problem

$$\theta_j := \arg \min_{\boldsymbol{\theta} \in \mathbb{R}^p} R_j(\boldsymbol{\theta}) = \arg \min_{(\boldsymbol{\gamma}, \boldsymbol{\xi}) \in \mathbb{R}^{p\Lambda} \times \mathbb{R}^{p\Pi}} d_M^2(f_j, \Lambda_{\boldsymbol{\gamma}} \circ f_0 \circ \Pi_{\boldsymbol{\xi}}^{-1}). \quad (10)$$

Note that the parameters θ_j obtained by solving problem (10) do not necessarily coincide (and in general do not) with the parameter values obtained by solving (9). The reason besides that is that in the later problem, the purpose is to optimally register curve f_j as a deformation of f_0 while in the previous problem is to optimally register f_0 to all curves in \mathcal{F} , so the qualitative difference is clear. However, repeating the registration procedure described in (10) for each $f_j \in \mathcal{F}$ one obtains the IC data sets $\{(\Lambda_j, \Pi_j)\}_{j=1}^n$ and $\{\boldsymbol{\theta}_j = (\boldsymbol{\gamma}_j, \boldsymbol{\xi}_j)'\}_{j=1}^n$ which provide information regarding the acceptable deviation levels from the mean curve characteristics either in functional

or parametric form. In fact, due to the centrality conditions, one can quantify the total deviance in amplitude or phase of each function f_j , according to a metric sense $d(\cdot)$, by calculating the differences $d(\Lambda_j, Id)$ and $d(\Pi_j, Id)$ and working with the inferred probability distributions. The same task can be done in terms of the parameters θ_j . In the following section we develop a monitoring approach for the under study framework relying on the information obtained by exactly these datasets.

3.2 An EWMA-type control chart for functional data

Following the characterization of the IC behaviour in Section 3.1 through the notion of Fréchet mean and the deformation models framework, we propose the construction of an EWMA-type chart for detecting shifts from the IC standard. We focus our interest on the case of curves representing the evolution of a quantity in a specified time interval $t \in I$, whose shape can be efficiently calibrated by the amplitude-phase deformation model discussed above. The rationale behind the proposed control chart, is similar to the classical EWMA charts procedure either for monitoring the process mean or variability of the statistical quantity under study (see e.g. Montgomery (2009)).

3.2.1 Fully non-parametric approach

Under a fully non-parametric approach, one can construct an EWMA-type control chart appropriately modified in order to be in line with the notion of Fréchet mean, and therefore compatible with the possibly non-linear structure of the space where the monitoring objects belong to. For example, in the case of curves $f_j \in M$, and under the assumption that the Fréchet mean is calculated with respect to the d_M metric, an EWMA-type chart definition is possible as

$$\tilde{f}_j = FM(f_j, \tilde{f}_{j-1}; \lambda, 1 - \lambda), \quad \lambda \in (0, 1), \quad j = 1, 2, \dots \quad (11)$$

where \tilde{f}_0 is defined as the Fréchet mean between the IC curves of the training set, $FM(g, h; \lambda, 1 - \lambda)$ denotes the Fréchet mean between the objects g and h with respective weights λ and $1 - \lambda$ while $\lambda \in (0, 1)$ denotes the sensitivity parameter of the chart. Depending on the application, the chosen metric may reveal different aspects of deviance of the monitoring objects from the IC state. While as standard choices may be used any L^q distance, the use of more complicated metrics depending on what type of deviance is considered as critical, may take into account more characteristics regarding the elements' nature during the determination of their respective mean. Observe that in the particular case where the L^q metric is used for $q = 2$ the occurring

chart gets

$$\tilde{f}_j = \lambda f_j + (1 - \lambda)\tilde{f}_{j-1}, \quad j = 1, 2, \dots \quad (12)$$

which coincides in formulation with the typical EWMA chart. However, the resulting chart element in this case is not a point but a new object \tilde{f}_j (curve in our case). As a result, any attempt to illustrate directly the chart elements may be unpractical for the monitoring purposes. Moreover, no other important information regarding other aspects/features of the process can be displayed by such a chart.

Since the aim of the discussed approach is to monitor the deviance of the process from the IC standard, it is reasonable to construct a chart with respect to the deviance of \tilde{f}_j from the IC profiles Fréchet mean, i.e. a chart for monitoring the process variability. Two alternatives can be considered here. The first one is a generalization of the standard EWMA variability chart and can be constructed in the following manner. Let us denote by $D_j = d_M^2(f_j, \tilde{f}_{j-1})$ where \tilde{f}_{j-1} denotes the estimated IC mean shape before the record of the observation j . Then, a chart for the variability process is the following

$$\tilde{D}_j = \lambda D_j + (1 - \lambda)\tilde{D}_{j-1}, \quad j = 1, 2, \dots \quad (13)$$

where as \tilde{D}_0 can be set the mean of the quadratic deviations of all the IC observations from the mean with respect to the metric d_M is used. Another option for the variability chart is to set as D_j the Fréchet function defined by the IC train set of curves with respect to the new element of the chart, i.e. $D_j = \frac{1}{n} \sum_{k=1}^n d_M^2(\tilde{f}_j, f_k^{IC})$. Therefore, the later chart will provide a shift if the Fréchet function significantly changes after the updated Fréchet mean estimation.

However, it is clear that the main disadvantage of the fully non-parametric approach is that shifts are detected without being able to further investigate the reason which lead to them, i.e. which particular characteristic(s) significantly deviates from the IC standard. That is the additive value the use of the deformation models offer in the monitoring task. In the following, a semi-parametric variation of the chart described in (11)-(13) is proposed, which provides additional evidence regarding the significant shifts in order to properly characterize the shift type and causality.

3.2.2 The general deformation modeling approach for monitoring nonlinear profiles

We employ now the amplitude-phase deformation model in order to provide a more complete monitoring mechanism for nonlinear functional profiles. Given a set of IC data $\{f_1, \dots, f_n\}$ the

IC typical shape f_0 is estimated through the procedure already described in Section 3.1 under the assumption that any IC element is acceptably deviant from the mean shape f_0 with respect to the amplitude-phase deformation model, i.e.

$$f_j = \Lambda_j \circ f_0 \circ \Pi_j^{-1} + \epsilon_j \quad (14)$$

where the remaining process $\epsilon_j(t)$ is considered as white noise. Being *acceptably deviant* means that the aggregate deformation occurred by both amplitude and phase deformaters Λ_j and Π_j does not exceed the deviance levels observed from the IC dataset. So, we need to investigate if a newly sampled element f_j is characterized as an *out-of-control* (OOC) one, which deformation is beyond the acceptable limits and of course to define that limits.

Since the IC behaviour f_0 has been derived by the IC dataset as described in Section 3.1, then for a newly sampled f_j one has first to derive the best model according to (14), i.e. to solve the related *registration problem* which in variational formulation is stated as

$$(\Lambda_j, \Pi_j) := \arg \min_{\Lambda, \Pi} d_M^2(f_j, \hat{f}(\Lambda, \Pi)) \quad (15)$$

where $\hat{f}(\Lambda, \Pi) := \Lambda \circ f_0 \circ \Pi^{-1}$ and Λ_j, Π_j are the corresponding deformation operators of f_j with respect to the IC standard f_0 , i.e. the deformation model that can best represent f_j as an amplitude-phase distortion of f_0 .

Similar to the fully non-parametric approach described in (11), we need to design a similar EWMA-type monitoring procedure. However, in this case the chart element \tilde{f}_j is decomposed to the amplitude and phase deformaters $\tilde{\Lambda}_j$ and $\tilde{\Pi}_j$ (remember that we need to model $\tilde{f}_j = \tilde{\Lambda}_j \circ f_0 \circ \tilde{\Pi}_j^{-1}$) which are obtained as the minimizers of the variational problem

$$(\tilde{\Lambda}_j, \tilde{\Pi}_j) := \arg \min_{\Lambda, \Pi} \lambda d_M^2(\Lambda \circ f_0 \circ \Pi^{-1}, \Lambda_j \circ f_0 \circ \Pi_j^{-1}) + (1 - \lambda) d_M^2(\Lambda \circ f_0 \circ \Pi^{-1}, \tilde{\Lambda}_{j-1} \circ f_0 \circ \tilde{\Pi}_{j-1}^{-1}) \quad (16)$$

for $j = 1, 2, \dots$ where $\tilde{\Lambda}_0 = Id$ and $\tilde{\Pi}_0 = Id$. Solving the later problem is equivalent to solving the problem (11) since the optimal deformaters pair $(\tilde{\Lambda}_j, \tilde{\Pi}_j)$ defines the optimizer of (11) under the deformation model (14), i.e. $\tilde{f}_j = \tilde{\Lambda}_j \circ f_0 \circ \tilde{\Pi}_j^{-1}$. From this point, since determination formulas for the elements $\tilde{f}_j, \tilde{\Lambda}_j, \tilde{\Pi}_j$ have been provided, one can use the monitoring procedure described in Section 3.2.1 in order to monitor either the whole process, or amplitude deformation process or phase deformation process separately depending on the purposes of the user.

Below we discuss some special cases for $(M, d_M) = (L^2, \|\cdot\|_2)$ (M is the set of deformation models) to make more clear the deformation modeling approach that is followed and the occurring

EWMA-type charts.

Example 3.1. In the special case where the curves f_j are members of the space L^2 and endowing the space with the usual euclidean metric ($d_M = \|\cdot\|_2$) by applying the above procedure, one gets the chart elements through the equation

$$\tilde{f}_j = \lambda \left(\Lambda_j \circ f_0 \circ \Pi_j^{-1} \right) + (1 - \lambda) \left(\tilde{\Lambda}_{j-1} \circ f_0 \circ \tilde{\Pi}_{j-1}^{-1} \right), \quad j = 1, 2, \dots \quad (17)$$

Therefore, in this case the chart coincides with the typical EWMA formulation (although there are no points here but functional objects) and the monitoring process for f_j can be applied as in the fully non-parametric case described in the previous section. However, the amplitude deformation process and the phase deformation process chart elements cannot be explicitly calculated, and the variational problem (16) has to be solved in this case for the determination of the elements $\tilde{\Lambda}_j$ and $\tilde{\Pi}_j$.

Example 3.2 (*Only amplitude deformations*). Assume that only amplitude deformations are considered on f_0 , i.e. each f_j is modeled as $f_j = \Lambda_j \circ f_0 + \epsilon_j$. In this case, any shift detection is interpreted as a significant change in the amplitude deformation process with respect to f_0 . Then, a chart can be proposed for monitoring the amplitude deformation process, which by equation (17) and substituting Π_j and $\tilde{\Pi}_{j-1}$ with Id for any j , we get that

$$\tilde{\Lambda}_j = \lambda \Lambda_j + (1 - \lambda) \tilde{\Lambda}_{j-1} \quad (18)$$

with $\tilde{\Lambda}_0 = Id$ which is equivalent to the classical EWMA type but for functions. Since only amplitude deformations are considered, then the IC status of the object f_j may be determined only by monitoring the variability of the induced amplitude deformation process with the non-parametric approach described in Section 3.2.1.

Example 3.3 (*Only phase deformations*). Considering only phase deformations with respect to the IC shape then we get the model $f_j = f_0 \circ \Pi_j^{-1} + \epsilon_j$. Similarly as above, any shift detection in f_j is interpreted as significant change in the phase deformation process and it would suffice to determine the status of f_j if one monitors the induced phase deformation process. However, the construction of an EWMA-type chart for monitoring Π_j is not that straightforward as in the case of the amplitude deformation process. In this case, the chart element $\tilde{\Pi}_j$ (that should also agree with chart (17)) is computed by solving the variational root finding problem

$$f_0 \circ \tilde{\Pi}_j^{-1} = \lambda f_0 \circ \Pi_j^{-1} + (1 - \lambda) f_0 \circ \tilde{\Pi}_{j-1}^{-1} \quad (19)$$

where $\tilde{\Pi}_0 = Id$. Then, the IC status of the object f_j is determined only by monitoring the variability of the induced phase deformation process with the non-parametric approach described in Section 3.2.1.

Example 3.4 (*Both amplitude and phase deformations*). In the case of both types of deformations, each f_j is modeled as $f_j = \Lambda_j \circ f_0 \circ \Pi_j^{-1} + \epsilon_j$. In general, even in the quadratic case ($q = 2$), an explicit derivation of charts that monitor amplitude and phase related to the EWMA chart for f_j is not possible (except the case where no phase deformation is considered). Clearly, the chart elements $\tilde{\Lambda}_j, \tilde{\Pi}_j$ should be obtained as the minimizers of the variational problem

$$\min_{\Lambda, \Pi} \left\{ \lambda \|\Lambda \circ f_0 \circ \Pi^{-1} - \Lambda_j \circ f_0 \circ \Pi_j^{-1}\|_2^2 + (1 - \lambda) \|\Lambda \circ f_0 \circ \Pi^{-1} - \tilde{\Lambda}_{j-1} \circ f_0 \circ \tilde{\Pi}_{j-1}^{-1}\|_2^2 \right\} \quad (20)$$

where Λ, Π are subject to certain monotonicity and boundary conditions. Clearly, only numerically solutions can be obtained. Then, the monitoring procedure is split into two parts: (a) monitoring the amplitude deformation process and (b) monitoring the phase deformation process through different variability charts similar to that discussed in Section 3.2.1. Then, by detecting a shift in the process f_j we can categorize further its type to amplitude-related or phase-related shift though the two charts for Λ_j and Π_j that accompany the proposed monitoring mechanism.

The variational problems (15) and (16) may prove quite challenging ones or computationally intractable depending on the nature of elements $f_j \in M$, the metric d_M used and the required conditions on the amplitude and phase deformaters (especially the second ones). Therefore, it is preferable in practice to use some parametric models for the deformaters Λ, Π (as already discussed in Section 3.1) which depend on some parameters $\theta = (\gamma, \xi) \in \mathbb{R}^p$. By this mean, the requirements for the deformaters are transformed to certain constraints regarding the parameter vector θ and the variational problem (15) is then simplified to the fitting problem

$$\theta_j := (\gamma_j, \xi_j) = \arg \min_{\theta \in \mathbb{R}^p} R_j(\theta) = \arg \min_{\theta \in \mathbb{R}^p} d_M^2(f_j, \hat{f}(\theta)) \quad (21)$$

where $\hat{f}(\theta) := \Lambda_\gamma \circ f_0 \circ \Pi_\xi^{-1}$ and γ_j, ξ_j denote the amplitude and phase deformation parameters characterizing (modeling) the amplitude and phase deformaters, respectively. Then, the parameter vector θ_j contains the optimal deformation parameters γ_j (amplitude) and ξ_j (phase), which characterize the respective deformation functions (i.e. $\Lambda_j := \Lambda(\cdot; \gamma_j)$ and $\Pi_j := \Pi(\cdot; \xi_j)$) and f_j can be best represented as a deformation of the Fréchet mean f_0 under the amplitude-phase deformation model (14).

Then, in order to estimate the chart elements \tilde{f}_j the EWMA-type chart elements are calcu-

lated as the Fréchet mean between the elements $\hat{f}_j := \hat{f}(\theta_j)$ and $\tilde{f}_{j-1} := \hat{f}(\tilde{\theta}_{j-1})$ with respective weights λ and $1 - \lambda$ assuming that \tilde{f}_j can be modeled by (14). Then, the Fréchet mean problem estimation is equivalent to solving the fitting problem

$$\tilde{\theta}_j := (\tilde{\gamma}_j, \tilde{\xi}_j) = \arg \min_{\theta \in \mathbb{R}^p} \tilde{R}_j(\theta) = \arg \min_{\theta \in \mathbb{R}^p} \{\lambda d_M^2(\hat{f}(\theta), \hat{f}_j) + (1 - \lambda) d_M^2(\hat{f}(\theta), \tilde{f}_{j-1})\} \quad (22)$$

Clearly, the minimizers of (22) determine the deformaters $\tilde{\Lambda}_j = \Lambda(\cdot; \tilde{\gamma}_j)$ and $\tilde{\Pi}_j = \Pi(\cdot; \tilde{\xi}_j)$ which are then used to estimate the element $\tilde{f}_j = \tilde{\Lambda}_j \circ f_0 \circ \tilde{\Pi}_j^{-1}$ for the EWMA-type chart. Therefore, the procedure for the construction of a EWMA-type chart for f_j based on the Fréchet mean and amplitude-phase deformation model framework can be briefly described by the following steps:

0. Given an IC dataset determine the Fréchet mean f_0 following the procedure described in 3.1.
1. Given a newly sampled $f_j \in M$ and the Fréchet mean f_0 of the IC dataset, determine the optimal deformation parameters θ_j by solving (21).
2. Determine $\tilde{\theta}_j$ for $j = 1, 2, \dots$ (setting $\tilde{\theta}_0$ such that satisfying the appropriate centrality conditions with respect to f_0) through the solution of problem (22).
3. Set $\tilde{f}_j := \hat{f}(\tilde{\theta}_j)$, for $j = 1, 2, \dots$ with $\tilde{f}_0 = f_0$ and estimate the variability chart element \tilde{D}_j according to the procedure described in (13) in order to detect significant shifts from f_0 . For any newly sampled f_j , repeat the steps from 1 to 3 while the IC standard f_0 is still valid.

The minimizers of problem (22) play the most important role in the monitoring procedure since we need these to define the chart elements for every possible characteristic of interest. The minimizing vector $\tilde{\theta}_j$ can be first used as a monitoring tool for the state of the process under study by paying special attention only to the deformation parameters. Then, EWMA-type charts can be constructed for the amplitude and phase deformaters through the elements $\tilde{\Lambda}_j$ and $\tilde{\Pi}_j$ since they directly depend on $\tilde{\theta}_j$. Finally, the whole process is monitored through the elements \tilde{f}_j . However, except the chart for the deformation parameters, the rest must be accompanied with charts for monitoring their respective variance (as described in Section 3.2.1 in order to reach to a conclusion regarding the shift status of each process.

Remark 3.5. One may consider to begin the monitoring procedure by building EWMA on the deformation parameters and then extending this chart for the deformation processes and then at the monitoring object f_j . However, non-linearity of f_j does not allow such an extension. Notice

that even in the case where both deformation functions Λ, Π are linear, e.g. $\Lambda(z) = az + b$, $\Pi(s) = cs + d$, although one may attempt to monitor the deformation functions separately, e.g. $\tilde{\Lambda}_j = \lambda\Lambda_j + (1 - \lambda)\tilde{\Lambda}_{j-1}$ and $\tilde{\Pi}_j = \lambda\Pi_j + (1 - \lambda)\tilde{\Pi}_{j-1}$, then the resulting chart for f_j through $\tilde{f}_j = \lambda\tilde{\Lambda}_j \circ f_0 \circ \tilde{\Pi}_j + (1 - \lambda)\tilde{f}_{j-1}$ does not coincide with the minimizer of equation (16).

3.3 The case of the shape-invariant deformation model

In order to better describe the monitoring procedure discussed in this section, we discuss as a particular case of great interest, the case where any shape deformation from the IC standard is quantified/parameterized by the shape invariant model (SIM) under the assumption that $f_j \in L^2$ and $d_M = \|\cdot\|_2$. This shape modeling approach has been repeatedly discussed and extended in the functional modeling literature (see e.g. Kneip & Engel (1995); Gervini & Gasser (2004); Bigot et al. (2013)). In this setting, each object f_j is modeled as a distortion of the IC standard f_0 (i.e. the mean behaviour of the IC objects) through the relation

$$f_j(t) = \beta_j + \alpha_j f_0\left(\frac{t - \zeta_j}{\kappa_j}\right) + \epsilon_j(t), \quad t \in I \quad (23)$$

which can be also realized as a special case of the amplitude-phase deformation model where $\Lambda_j(z) = \alpha_j z + \beta_j$ and $\Pi(s) = \kappa_j s + \zeta_j$ with (α_j, β_j) denote the deformation parameters on the scale and location on the process' amplitude, while (κ_j, ζ_j) denote the deformation parameters on the scale and location on the process' phase. In other words, we realize \mathcal{M} as the subset of L^2

$$\mathcal{M} := \left\{ f \in L^2 : \exists (\alpha, \beta, \kappa, \zeta)' \in \mathbb{R}^4 \text{ such that } f(t) = \beta + \alpha f_0\left(\frac{t - \zeta}{\kappa}\right), \quad t \in I \right\}$$

Following the functional monitoring approach described in Sections 3.1 and 3.2, assuming that there is available a set of IC curves $\mathcal{F} = \{f_1, \dots, f_n\} \in \mathcal{M} \subset L^2$, we estimate the corresponding Fréchet mean (i.e. the IC standard). By directly substituting the above linear amplitude and phase deformation parametric models to equation (8) we obtain the following semi-parametric representation of the Fréchet mean:

$$\hat{f}_{IC}(t; \boldsymbol{\theta}) = \frac{1}{n} \sum_{j=1}^n \left\{ \alpha_j^{-1} f_j\left(\frac{t + \zeta_j}{\kappa_j}\right) - \alpha_j^{-1} \beta_j \right\} \quad (24)$$

which depends on the vector of deformation parameters

$$\boldsymbol{\theta} := (\boldsymbol{\alpha}, \boldsymbol{\beta}, \boldsymbol{\kappa}, \boldsymbol{\zeta})' = (\alpha_1, \dots, \alpha_n, \beta_1, \dots, \beta_n, \kappa_1, \dots, \kappa_n, \zeta_1, \dots, \zeta_n)' \in \mathbb{R}^{4n}.$$

The optimal parameter vector that characterize the respective Fréchet mean is chosen through the solution of the optimization problem (Fréchet function minimization)

$$\boldsymbol{\theta}_* = \arg \min_{\boldsymbol{\theta} \in \mathfrak{D}} \frac{1}{n} \sum_{j=1}^n \|f_j - \hat{f}_{IC}(\boldsymbol{\theta})\|_2^2, \quad (25)$$

where $\mathfrak{D} \subset \mathbb{R}^{4n}$ denotes the parametric space on which feasible solutions of (25) are contained, satisfying the centrality requirements

$$\prod_{j=1}^n \alpha_j^{1/n} = 1, \quad \sum_{j=1}^n \beta_j = 0, \quad \prod_{j=1}^n \kappa_j^{1/n} = 1, \quad \sum_{j=1}^n \zeta_j = 0$$

in order to satisfy the deformaters' centrality properties $\mathbb{E}[\Lambda] = Id$ and $\mathbb{E}[\Pi] = Id$. Then, we set as IC standard the curve $f_0 := \hat{f}_{IC}(\boldsymbol{\theta}_*)$. Next, for any newly sampled f_j we follow the procedure, discussed in Section 3.2.2. For a newly sampled f_j a registration step is performed, in order to model the curve f_j as a shape-invariant deformation of f_0 (with respect to the formulation (23)), through the related registration problem

$$\boldsymbol{\theta}_j = (\alpha_j, \beta_j, \kappa_j, \zeta_j) = \arg \min_{\boldsymbol{\theta} \in \mathbb{R}^4} \|f_j - \hat{f}(\boldsymbol{\theta})\|_2^2 \quad (26)$$

where $\hat{f}(\boldsymbol{\theta}) = \beta + \alpha f_0 \left(\frac{t-\zeta}{\kappa} \right)$.

Let us denote $\hat{f}_j := \hat{f}(\boldsymbol{\theta}_j)$. Then we construct the EWMA-type chart on f_j using the assumed shape parameterization, which elements \tilde{f}_j are chosen as the Fréchet barycenter between \hat{f}_j and \tilde{f}_{j-1} with weights λ and $1 - \lambda$ respectively, i.e. through the fitting problem

$$\tilde{\boldsymbol{\theta}}_j := \arg \min_{\boldsymbol{\theta} \in \mathbb{R}^4} \lambda \|\hat{f}(\boldsymbol{\theta}) - \hat{f}_j\|_2^2 + (1 - \lambda) \|\hat{f}(\boldsymbol{\theta}) - \tilde{f}_{j-1}\|_2^2 \quad (27)$$

where $\tilde{f}_{j-1} := \hat{f}(\tilde{\boldsymbol{\theta}}_{j-1})$ and $\tilde{\boldsymbol{\theta}}_0 = (\tilde{\alpha}_0, \tilde{\beta}_0, \tilde{\kappa}_0, \tilde{\zeta}_0) = (1, 0, 1, 0)$. Setting $\tilde{f}_j := \hat{f}(\tilde{\boldsymbol{\theta}}_j)$ we construct an EWMA chart for monitoring variability of the process as proposed in equation (13). Then, even if shift not detected for the whole process, EWMA-type charts can be constructed for monitoring the variability of amplitude deformation and phase deformation processes through their affine parametric forms. Of course, EWMA-type charts can be also build for each shape deformation parameter separately since each one quantifies different feature of deviance from the IC standard. However, potential shift detections on the shape distortion parameters depicted in the EWMA charts do not necessarily lead to a shift of the corresponding curve under study. However, shift detection on at least one of the deformation processes should lead to a shift of the curve. The procedure is briefly described below.

Algorithm 3.6. *Monitoring scheme for functional profiles under the shape invariant model*

Phase I: *Determination of the IC behaviour and acceptable levels of deviance*

Step 0 Provide as input a set of IC curves $\{f_1, f_2, \dots, f_n\}$.

Step 1 Estimate the Fréchet mean curve f_0 from the IC data and the related IC set of deformation parameters $\left\{\theta_j^{IC} = (\alpha_j^{IC}, \beta_j^{IC}, \zeta_j^{IC}, \kappa_j^{IC})'\right\}_{j=1}^n$.

Phase II: *EWMA-type chart construction and detection of possible shifts from the IC standard*

Step 2 Given a newly sampled curve f_j register it to the SIM deformation model with respect to f_0 by solving problem (26) and obtain the deformation parameters θ_j and set $\hat{f}_j := \hat{f}(\theta_j)$.

Step 3 Calculate the component \tilde{f}_j of the EWMA-type chart through the solution of the problem (27) and then calculate the j -th component for the EWMA-type variability monitoring chart as proposed in (13).

- If shift detected, then characterize the curve as OOC and further investigate the reason of the shift by applying relevant EWMA-type charts for the deformation parameters $\tilde{\theta}_j$ (or the resulting deformaters) calculated through (27).
- If no shift detected, then characterize the curve as IC and enrich the IC databank with the parameters $\tilde{\theta}_j$.

Step 4 Repeat Steps 2-3 for any newly sampled curve.

3.4 Numerical Schemes for the Monitoring Procedure

In this subsection we discuss the numerical approximation of the optimization problems (25), (26) and (27) related to the proposed monitoring process for functional profiles. These problems concern the determination of the Fréchet mean of the IC curves, the modeling of newly obtained data (curves) as shape-invariant deformations of the mean curve and the estimation of the EWMA-type chart elements. We will discuss each optimization problem separately as it occurs.

First, we treat the Fréchet mean estimation problem (25) for the IC data curves. For convenience, let us denote the objective function of the problem as

$$V(\gamma, \xi) := \frac{1}{n} \sum_{j=1}^n \int_I (f_j(t) - \hat{f}_{IC}(t; \gamma, \xi))^2 dt \quad (28)$$

where \hat{f}_{IC} is defined in (24), $\gamma = (\bar{\alpha}, \beta)'$ (with $\bar{\alpha} := \alpha^{-1}$) denotes the vector of amplitude deformation parameters and $\xi = (\kappa, \zeta)'$ denotes the vector of phase distortion parameters. Splitting the parameters into two distinct groups is extremely important for the development

of an efficient numerical scheme. Observe that, in the absence of the parameter centrality constraints, the function V depends quadratically on the parameter vector γ (after the substitution of α with $\bar{\alpha}$) while as far as the parameter vector ξ is concerned the dependence is fully non-quadratic and importantly non-convex on the parameter vector ξ . Therefore, treating the problem with respect to all the parameters simultaneously results to a non-convex minimization problem which is computationally quite expensive. Instead, we propose an iterative two-stage minimization scheme which exploits the quadratic dependence of the problem on the amplitude deformation parameters γ . Let us consider the parameter spaces Θ_Λ , Θ_Π

$$\Theta_\Lambda = \left\{ \gamma = (\bar{\alpha}, \beta)' \in \mathbb{R}^{2n} : \prod_{j=1}^n \bar{\alpha}_j^{1/n} = 1, \sum_{j=1}^n \beta_j = 0, \bar{\alpha}_j > 0, \forall j = 1, 2, \dots, n \right\}$$

$$\Theta_\Pi = \left\{ \xi = (\kappa, \zeta)' \in \mathbb{R}^{2n} : \prod_{j=1}^n \kappa_j^{1/n} = 1, \sum_{j=1}^n \zeta_j = 0, \zeta_j \in \left[-\frac{1}{2}, \frac{1}{2}\right], \forall j = 1, 2, \dots, n \right\}$$

for the amplitude deformation and phase deformation parameters respectively. The following two-stage minimization scheme is proposed:

Algorithm 3.7. *Two-stage iterative numerical scheme for the Fréchet mean estimation under the shape invariant model*

Step 0 Set $k = 1$, $\gamma^{(0)} = (1, 1, \dots, 1, 0, 0, \dots, 0)'$, $\xi^{(0)} = (1, 1, \dots, 1, 0, 0, \dots, 0)'$ and define the tolerance level ($\epsilon > 0$).

Step 1 Solve the unconstrained quadratic optimization problem $\hat{\gamma} = \arg \min_{\gamma \in \mathbb{R}^{2n}} V(\gamma, \xi^{(k-1)})$ and then compute the projection $\gamma^{(k)} = Proj_{\Theta_\Lambda}(\hat{\gamma})$

Step 2 Solve the unconstrained nonconvex optimization problem $\hat{\xi} = \arg \min_{\xi \in \mathbb{R}^{2n}} V(\gamma^{(k)}, \xi)$ and then compute the projection $\xi^{(k)} = Proj_{\Theta_\Pi}(\hat{\xi})$

Step 3 If $\|\gamma^{(k)} - \gamma^{(k-1)}\| < \epsilon$ and $\|\xi^{(k)} - \xi^{(k-1)}\| < \epsilon$ stop and set $(\gamma_*, \xi_*) = (\gamma^{(k)}, \xi^{(k)})$. Else set $k = k + 1$ and go to *Step 1*.

Clearly, the parameter vector $(\gamma_*, \xi_*) \in \Theta_\Lambda \times \Theta_\Pi$ determines the Fréchet mean of the data under study. At Step 1, the solution of the unconstrained quadratic minimization problem can be derived explicitly and then the projection to the parameter space Θ_Λ can be treated effectively by any gradient-descent type scheme. At Step 2, the unconstrained nonlinear (non-convex) minimization problem is quite difficult to handle effectively by gradient-based algorithms. Therefore, the use of an evolutionary optimization method (like Simulated Annealing or Particle Swarm Optimization) is recommended here in order to avoid local minima of the

problem. The projection to the parameter space Θ_{Π} can be efficiently treated as in Step 1 by any gradient-based scheme (since this problem is strongly convex with respect to ξ). The terminal condition in Step 3 guarantees the convergence of the problem to the minimum value of $V(\gamma, \xi)$ due to the continuity with respect to the problem parameters. The above two-stage iterative scheme generates a sequence of points $\{\theta_k\}_k$ by alternating projections between two convex sets. In fact, at Step 1 the problem is solved on the convex set $\Gamma := \Theta \times \mathbb{R}^{2n}$ generating a sequence of points $\{\bar{\theta}_k\}_k \subset \Gamma$, while at Step 2, the problem is solved on the convex set $\Xi := \mathbb{R}^{2n} \times \Theta_{\Pi}$ generating a sequence of points $\{\tilde{\theta}_k\}_k \subset \Xi$. It can be shown by the alternating projections algorithm (see e.g. Bauschke & Borwein (1993, 1994)) that as k grows, both sequences converge to a point θ_* in the intersection of the two sets $\mathcal{D} = \Gamma \cap \Xi$, being the minimizer of $V(\theta)$.

Next we discuss the registration problem (26). Since the Fréchet mean have been determined as $f_0 := \hat{f}_{IC}(\theta_*)$ the next crucial step for the monitoring procedure is the determination of the deformation parameters with respect to the IC standard f_0 . Assuming that the values of the phase deformation parameters κ, ζ are known, the optimal values for the amplitude deformation parameters can be derived in analytical form and in particular

$$\alpha_*(\kappa, \zeta) = \frac{\int_I f_0 \left(\frac{t-\zeta}{\kappa} \right) f_j(t) dt - \int_I f_0 \left(\frac{t-\zeta}{\kappa} \right) dt \int_I f_j(t) dt}{\int_I f_0^2 \left(\frac{t-\zeta}{\kappa} \right) dt - \left(\int_I f_0 \left(\frac{t-\zeta}{\kappa} \right) dt \right)^2} \quad (29)$$

$$\beta_*(\kappa, \zeta) = \int_I f_j(t) dt - \alpha_*(\kappa, \zeta) \int_I f_0 \left(\frac{t-\zeta}{\kappa} \right) dt. \quad (30)$$

This fact, allows us to rewrite the problem (26) to a reduced form depending only on the phase deformation parameters (κ, ζ) . However, the resulting problem is a fully non-quadratic and non-convex problem with respect to the phase deformation parameters and therefore any gradient-based scheme has high chances to fail in locating the minima. As a result, any evolutionary minimization method offers an easy way out especially because the low dimension of the problem.

Finally, the EWMA-type chart element estimation problem expressed in (27) can be treated similarly to (26) since the optimal amplitude deformation parameters can be analytically ex-

pressed as functions of the phase deformation parameters:

$$\begin{aligned} \tilde{\alpha}_*(\tilde{\kappa}, \tilde{\zeta}) &= \frac{\lambda \left(\int_I f_0 \left(\frac{t-\tilde{\zeta}}{\tilde{\kappa}} \right) \hat{f}_j(t) dt - \int_I f_0 \left(\frac{t-\tilde{\zeta}}{\tilde{\kappa}} \right) dt \int_I \hat{f}_j(t) dt \right)}{\int_I f_0^2 \left(\frac{t-\tilde{\zeta}}{\tilde{\kappa}} \right) dt - \left(\int_I f_0 \left(\frac{t-\tilde{\zeta}}{\tilde{\kappa}} \right) dt \right)^2} \\ &+ \frac{(1-\lambda) \left(\int_I f_0 \left(\frac{t-\tilde{\zeta}}{\tilde{\kappa}} \right) \tilde{f}_{j-1}(t) dt - \int_I f_0 \left(\frac{t-\tilde{\zeta}}{\tilde{\kappa}} \right) dt \int_I \tilde{f}_{j-1}(t) dt \right)}{\int_I f_0^2 \left(\frac{t-\tilde{\zeta}}{\tilde{\kappa}} \right) dt - \left(\int_I f_0 \left(\frac{t-\tilde{\zeta}}{\tilde{\kappa}} \right) dt \right)^2} \end{aligned} \quad (31)$$

$$\tilde{\beta}_*(\tilde{\kappa}, \tilde{\zeta}) = \lambda \int_I \hat{f}_j(t) dt + (1-\lambda) \int_I \tilde{f}_{j-1}(t) dt - \tilde{\alpha}_*(\tilde{\kappa}, \tilde{\zeta}) \int_I f_0 \left(\frac{t-\tilde{\zeta}}{\tilde{\kappa}} \right) dt \quad (32)$$

Substituting the above relations into problem (27) a reduced form of the problem is obtained depending only on the phase parameters $(\tilde{\kappa}, \tilde{\zeta})$ which can be optimally chosen with the same minimization approach used in the aforementioned registration problem.

4 Illustration of the monitoring methods in real data: Air Pollution Monitoring

In this section, the functional monitoring methodology presented in Section 3 is employed in studying air pollution data collected from atmospheric pollution sensors installed in the area of Athens, by the Ministry of Environment and Energy. Specifically, the study concerns the monitoring of air pollution in the area of Patission Street for the time period 2004-2006. The available data consist of daily measurements (mean values per hour for the duration of a day, i.e. 24 measurements) regarding the concentration of quantities considered as potential pollutants and specifically the concentration of: carbon monoxide (CO), nitrogen monoxide (NO), nitrogen dioxide (NO₂), ozone (O₃) and sulfur dioxide (SO₂) measured in mg/m³. Certain safety concentration thresholds for the human health have been set according to the directions of the World Health Organization (WHO) (Table 1) which violation consists high risk for the human health. As a result, from the scope of WHO, a day which at least one of the thresholds has been violated is considered as an OOC day, while if none has been violated is considered as an IC day.

However, these limits are continuously revised, and it is obvious that this threshold approach is maybe not the better strategy for monitoring atmospheric pollution. In fact, these criteria become more and more conservative. The discussed monitoring approach in this work, can offer an alternative monitoring tool for such phenomena that involve simultaneously with similar manner (maybe with small fluctuations from a specific standard) and can additionally provide an effective modeling approach for characteristics that cannot be sufficiently captured by mean

Polluter	Safety Threshold (mg/m ³)
Carbon Monoxide (CO)	≤ 10 (mean value per 8 hours)
Nitrogen Monoxide (NO)	No specified limit
Nitrogen Dioxide (NO ₂)	≤ 400 (hourly mean value)
Ozone (O ₃)	≤ 240 (hourly mean value)
Sulfur Dioxide (SO ₂)	≤ 500 (hourly mean value)

Table 1: Safety concentration thresholds of the pollutants under study for human health according to the World Health Organization

values. In order to illustrate the capabilities of the discussed monitoring methodologies, we use as train dataset the measurements from year 2004 and as test datasets the measurements from the time period 2005-2006.

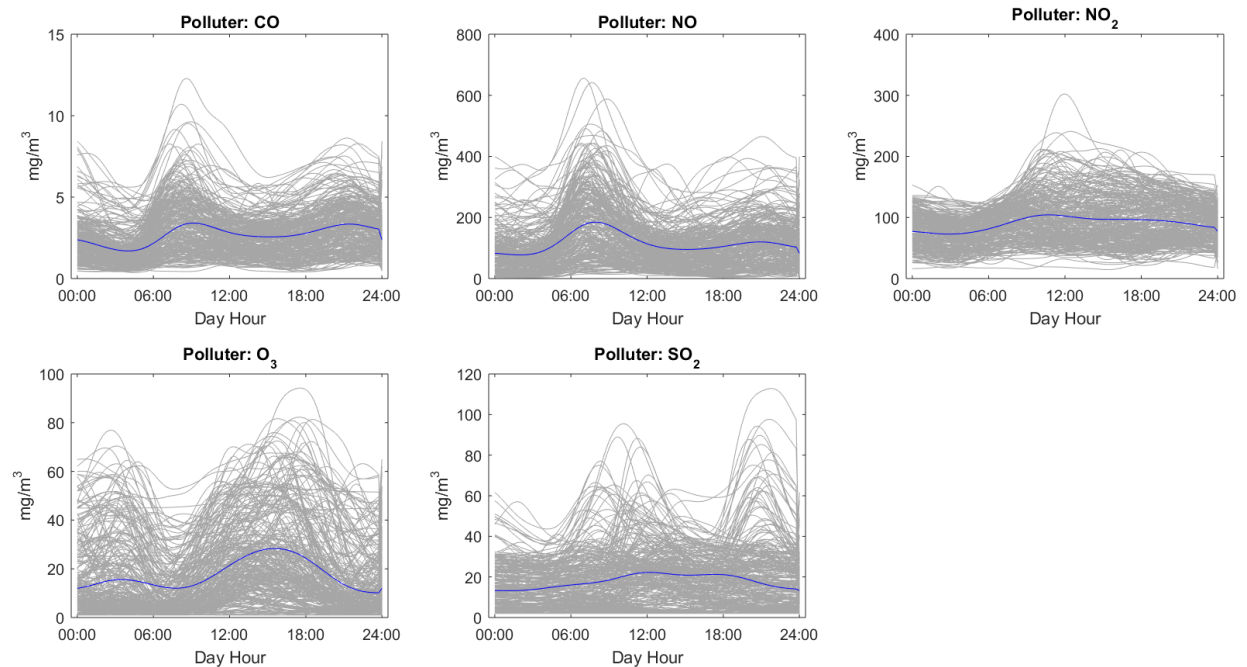


Figure 1: The calculated IC Fréchet mean curves (blue lines) for the intra-day (per hour) concentration of each one of the pollutants (CO, NO, NO₂, O₃, SO₂) in the regional atmosphere.

4.1 Phase I: Definition of the IC behaviour for the pollutants intra-day concentration

First, the Phase I of the monitoring procedure is performed using as a train dataset the IC observations from the year 2004, where the typical behaviour for the intra-day concentration of each pollutant is estimated (i.e. the typical shape of the daily evolution of each pollutant) and the empirical distributions of the deformation parameters indicating the acceptable levels of deviation from the typical curve. The shape invariant model is employed as a particular deformation model, presented and discussed in Section 3.3, however we omit the phase scaling parameter κ

in order to simplify the analysis. Clearly, the parameterization of certain characteristics of the data will allow for a more careful and meaningful monitoring of the changes that could possibly affect the air pollution status of each day (IC or OOC) in the region of interest.

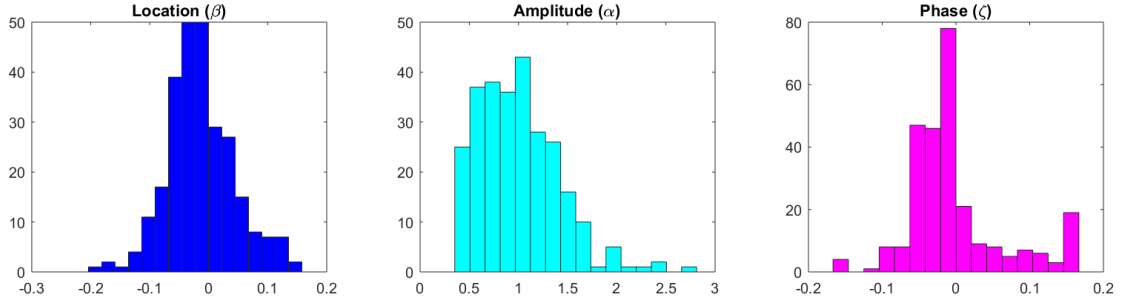


Figure 2: Distributions of the IC trainset deformation parameters for CO.

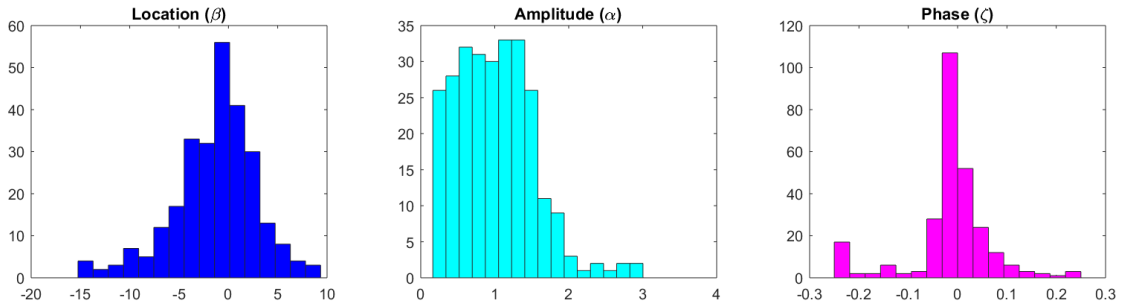


Figure 3: Distributions of the IC trainset deformation parameters for NO.

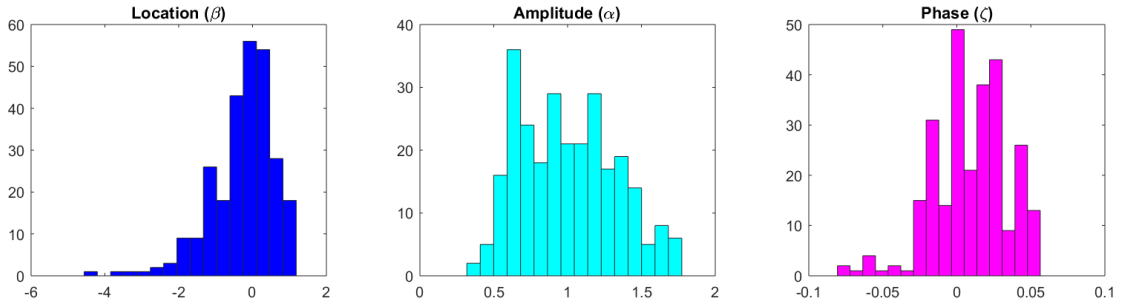


Figure 4: Distributions of the IC trainset deformation parameters for NO₂.

In Figure 1 are illustrated the IC daily curves from the train dataset and the estimated IC intra-day mean behaviour under the Fréchet mean notion for each pollutant under consideration. Clearly, the data shapes (intra-day pollutant concentration curves) seem to be successfully calibrated by the shape invariant model and the calculated Fréchet means are plausible representations of the typical behaviour of the pollutants' daily concentration curves. Subsequently, in Figures 2, 3, 4, 5 and 6 are illustrated the empirical distributions of the deformation parameters $\theta = (\beta, \alpha, \zeta)'$ as estimated from the IC trainset for each one of the pollutants under study. These distributions are used at a second stage as databanks for the monitoring and determination of

the deformation parameters control status since they contain valuable information regarding the acceptable levels of deviance from the IC standard.

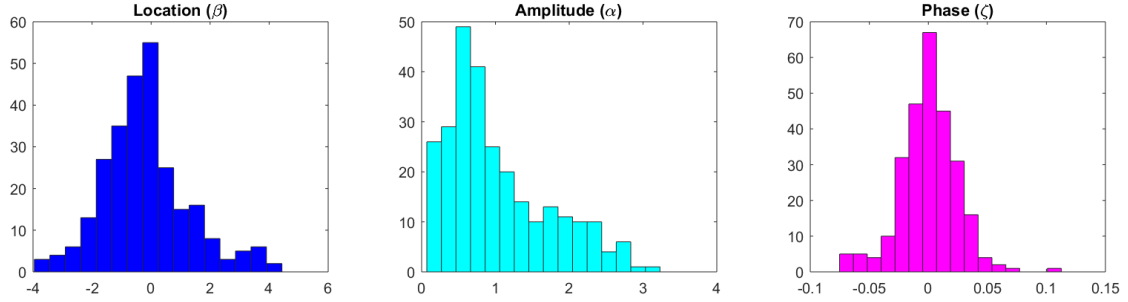


Figure 5: Distributions of the IC trainset deformation parameters for O_3 .

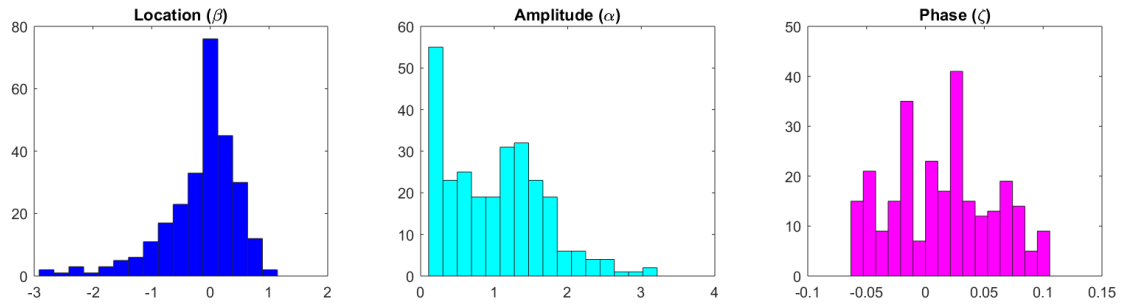


Figure 6: Distributions of the IC trainset deformation parameters for SO_2 .

4.2 Phase II: Determination of the control status for newly sampled curves

Next, the Phase II of the functional monitoring scheme is performed. The test dataset concerning the time period 2005-2006 is studied in order to illustrate the capabilities of the EWMA-type chart discussed in Section 3.3. Following the described procedure, EWMA charts for the sampled curves deviance from the IC standard are constructed in order to detect significant shifts. The EWMA charts for all pollutants are illustrated in Figures 7, 8, 9, 10 and 11 (last column). Note that the Fréchet mean is employed according to the L^2 -metric sense ($q = 2$), while the exponential weighting parameters that have been tested are $\lambda = 0.05, 0.10, 0.15, 0.20$ where the optimal choice was selected per case. Note here that investigating more cautiously the optimal choice for λ could further improve the performance of the method. Perhaps, a better strategy is to occasionally alternate the weighting parameter value depending on the application. Such a task could be done by separating the train set to further parts and cross-validating for the better choice of λ in different train sets. However, we feel that is beyond the scopes of this research work and therefore we use a constant value for each pollutant for the whole monitoring task. For the case of deviance monitoring only an upper control limit is applied based on the information from the IC data collected from the year 2004 (at 95% level). It seems that significant shift

detections are observed mainly for the pollutants CO, NO and SO₂ in Autumn and Winter, while shifts are detected for the pollutants NO₂ and O₃ mainly in Spring and Summer. This could be evidence of seasonality effects to the pollutants influence on the regional atmosphere of the city and correlation patterns to the evolution of each pollutant.

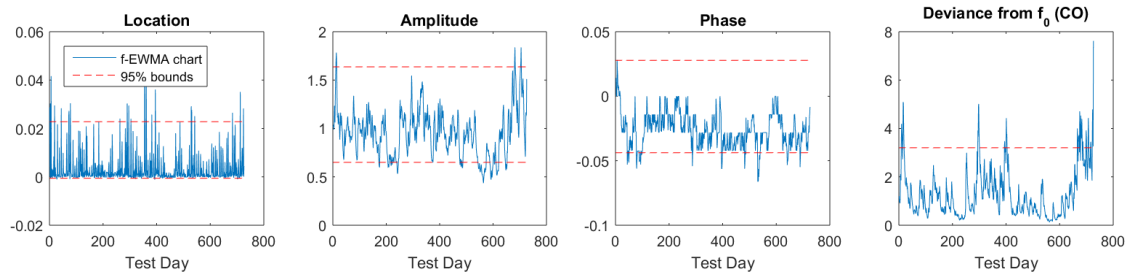


Figure 7: EWMA-type charts for monitoring the status of pollutant CO

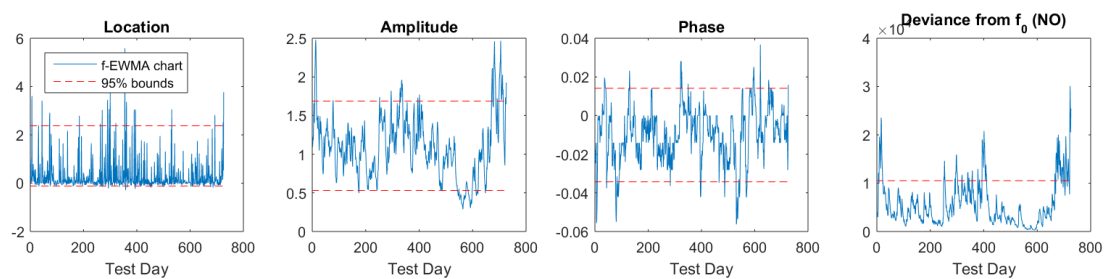


Figure 8: EWMA-type charts for monitoring the status of pollutant NO

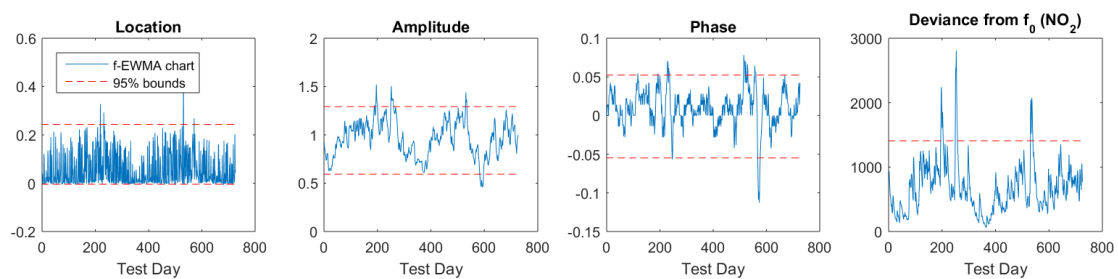


Figure 9: EWMA-type charts for monitoring the status of pollutant NO₂

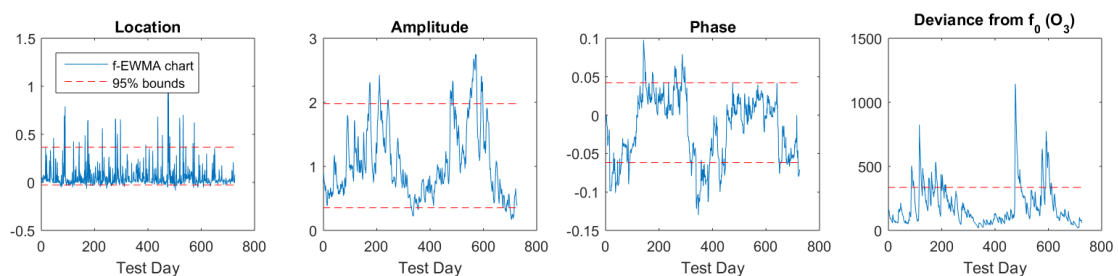


Figure 10: EWMA-type charts for monitoring the status of pollutant O₃

Additional information regarding the shifts can be extracted by the monitoring of the deformation parameters. In particular, in figures 7, 8, 9, 10 and 11 (first three columns) are illustrated

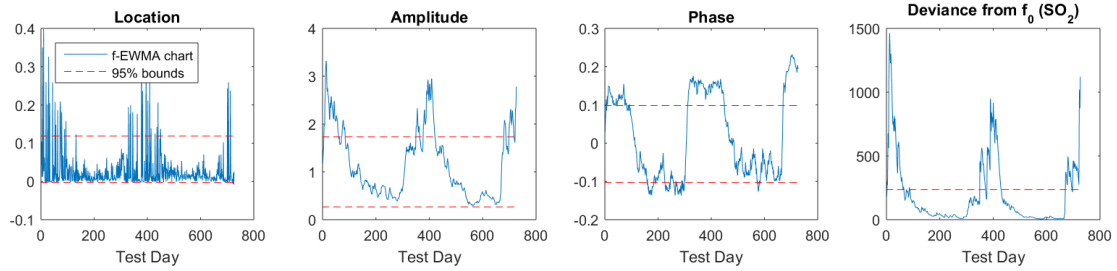


Figure 11: EWMA-type charts for monitoring the status of pollutant SO_2

the EWMA-type charts discussed in Section 3 for the deformation parameters β, α, ζ for each one of the pollutants under study. In general, the deformation parameters shift detections per pollutant are in line with the shift detections of the related curves. It is important to notice from these charts the variability and the shaped patterns which may lead to very interesting and useful interpretations for the pollutants behaviour under different conditions e.g., seasonality. In particular, the location and amplitude deformation parameters monitoring seems to be in line since in most cases provide significant shifts of the pollutant under study at the same time. The phase deformation parameter is also in line with the significant shifts in deviance from the IC behaviour, since in the occasions where a significant shift is observed is very possible to be combined with an out-of-control value for the phase parameter. It is important to observe that each pollutant present in general the same pattern in the estimated EWMA-type charts both in monitoring deviance from the IC standard, as well as in the location, amplitude and phase deformation parameters. This fact indicates that a very valid allocation of the total deviance to these special characteristics (location, amplitude and phase) has been performed by the monitoring procedure in combination with the shape-invariant model parameterization. However, one would also consider to repeat this approach to certain time windows (e.g., per season) in order to obtain more detailed IC behaviours in the windows of interest, where the shifts will be referred to the “local” IC behaviour e.g., the IC standard for Autumn or Winter.

5 Conclusions

In this work a framework for the statistical monitoring of functional data by combining the notion of the Fréchet mean and the framework of deformation models is proposed. In particular the amplitude-phase deformation model has been studied as a modeling approach of the functional profiles under study in order to represent each profile as a distortion of the typical profile that should be observed, i.e. the Fréchet mean of the profiles that are considered as in control. The combination of these frameworks offers (a) a computationally effective way to estimate the Fréchet mean since the computational cost is significantly reduced by transforming the related

optimization problems from variational to fitting ones, and (b) the approach of deformation models allows for allocating the deviance of complex objects like functional profiles to certain characteristics setting also as a reference standard the Fréchet mean. The particular case of the shape invariant model is discussed and applied in a case study for monitoring the air pollution in an area of the city of Athens with considerable success.

Acknowledgements

The authors wish to acknowledge for financial support from the research program DRASI II 2017-19 funded by the AUEB Research Center.

References

- Afsari, B. (2011). Riemannian l^p center of mass: existence, uniqueness and convexity. *Proceedings of the American Mathematical Society*, 139(2), 655–673.
- Arnaudon, M., Barbaresco, F., & Yang, L. (2013). Medians and means in Riemannian geometry: existence, uniqueness and computation. In *Matrix information geometry* (pp. 169–197). Springer.
- Bauschke, H. H., & Borwein, J. M. (1993). On the convergence of von neumann’s alternating projection algorithm for two sets. *Set-Valued Analysis*, 1(2), 185–212.
- Bauschke, H. H., & Borwein, J. M. (1994). Dykstra’s alternating projection algorithm for two sets. *Journal of Approximation Theory*, 79(3), 418–443.
- Bigot, J., Charlier, B., et al. (2011). On the consistency of fréchet means in deformable models for curve and image analysis. *Electronic Journal of Statistics*, 5, 1054–1089.
- Bigot, J., Gadat, S., & Loubes, J.-M. (2009). Statistical m-estimation and consistency in large deformable models for image warping. *Journal of Mathematical Imaging and Vision*, 34(3), 270–290.
- Bigot, J., Gendre, X., et al. (2013). Minimax properties of Fréchet means of discretely sampled curves. *The Annals of Statistics*, 41(2), 923–956.
- Cano, J., Moguerza, J. M., Psarakis, S., & Yannacopoulos, A. N. (2015). Using statistical shape theory for the monitoring of nonlinear profiles. *Applied stochastic models in business and industry*, 31(2), 160–177.

- Chicken, E., Pignatiello Jr, J. J., & Simpson, J. R. (2009). Statistical process monitoring of nonlinear profiles using wavelets. *Journal of Quality Technology*, *41*(2), 198–212.
- Chui, C. K. (2016). *An introduction to wavelets*. Elsevier.
- Dubey, P., & Müller, H.-G. (2019). Fréchet analysis of variance for random objects. *Biometrika*, *106*(4), 803–821.
- Fassò, A., Toccu, M., & Magno, M. (2016). Functional control charts and health monitoring of steam sterilizers. *Quality and Reliability Engineering International*, *32*(6), 2081–2091.
- Fréchet, M. (1948). Les éléments aléatoires de nature quelconque dans un espace distancié. In *Annales de l'institut Henri Poincaré* (Vol. 10, pp. 215–310).
- Gervini, D., & Gasser, T. (2004). Self-modelling warping functions. *Journal of the Royal Statistical Society: Series B (Statistical Methodology)*, *66*(4), 959–971.
- Goodall, C. (1991). Procrustes methods in the statistical analysis of shape. *Journal of the Royal Statistical Society: Series B (Methodological)*, *53*(2), 285–321.
- Izem, R., Marron, J. S., et al. (2007). Analysis of nonlinear modes of variation for functional data. *Electronic Journal of Statistics*, *1*, 641–676.
- Jung, S., Dryden, I. L., & Marron, J. (2012). Analysis of principal nested spheres. *Biometrika*, *99*(3), 551–568.
- Kampelis, N., Papayiannis, I. G., et al. (2020). An integrated energy simulation model for buildings. *Energies*.
- Kendall, D. G., Barden, D., Carne, T. K., & Le, H. (2009). *Shape and shape theory* (Vol. 500). John Wiley & Sons.
- Kneip, A., & Engel, J. (1995). Model estimation in nonlinear regression under shape invariance. *The Annals of Statistics*, 551–570.
- Kravvaritis, D. C., & Yannacopoulos, A. N. (2020). *Variational methods in nonlinear analysis: With applications in optimization and partial differential equations*. Walter de Gruyter GmbH & Co KG.
- Le, H., & Kume, A. (2000). The fréchet mean shape and the shape of the means. *Advances in Applied Probability*, 101–113.

- McGinnity, K., Chicken, E., & Pignatiello Jr, J. J. (2015). Nonparametric changepoint estimation for sequential nonlinear profile monitoring. *Quality and Reliability Engineering International*, *31*(1), 57–73.
- Moguerza, J. M., Muñoz, A., & Psarakis, S. (2007). Monitoring nonlinear profiles using support vector machines. In *Iberoamerican congress on pattern recognition* (pp. 574–583).
- Montgomery, D. C. (2009). *Statistical quality control* (Vol. 7). Wiley New York.
- Panaretos, V. M., Zemel, Y., et al. (2016). Amplitude and phase variation of point processes. *The Annals of Statistics*, *44*(2), 771–812.
- Papayiannis, G. I., Giakoumakis, E. A., et al. (2018). A functional supervised learning approach to the study of blood pressure data. *Statistics in medicine*, *37*(8), 1359–1375.
- Papayiannis, G. I., & Yannacopoulos, A. N. (2018). A learning algorithm for source aggregation. *Mathematical Methods in the Applied Sciences*, *41*(3), 1033–1039.
- Petersen, A., Müller, H.-G., et al. (2019). Fréchet regression for random objects with euclidean predictors. *The Annals of Statistics*, *47*(2), 691–719.
- Qiu, P., Zou, C., & Wang, Z. (2010). Nonparametric profile monitoring by mixed effects modeling. *Technometrics*, *52*(3), 265–277.
- Ramsay, J. O., & Silverman, B. W. (2007). *Applied functional data analysis: methods and case studies*. Springer.
- Shiau, J.-J. H., Huang, H.-L., Lin, S.-H., & Tsai, M.-Y. (2009). Monitoring nonlinear profiles with random effects by nonparametric regression. *Communications in Statistics?Theory and Methods*, *38*(10), 1664–1679.
- Small, C. G. (2012). *The statistical theory of shape*. Springer Science & Business Media.
- Wahba, G. (1990). *Spline models for observational data* (Vol. 59). SIAM.
- Wand, M. P., & Jones, M. C. (1994). *Kernel smoothing*. Chapman and Hall/CRC.
- Wang, K., Gasser, T., et al. (1997). Alignment of curves by dynamic time warping. *The annals of Statistics*, *25*(3), 1251–1276.
- Williams, J. D., Woodall, W. H., & Birch, J. B. (2007). Statistical monitoring of nonlinear product and process quality profiles. *Quality and Reliability Engineering International*, *23*(8), 925–941.